International Journal of Nanoelectronics and Materials
IJNeaM
ISSN 1985-5761 | E-ISSN 2232-1535

Computational Analysis on The Influence of Heterojunction Geometries to Electrical Performance of Photovoltaic Cells

Prasanna Dass[a], Nor Farhani Zakaria[a,b], Mohd Fairus Ahmad[a], Shahrir Rizal Kasjoo[a,c], Safizan Shaari[a,b], Shamsul Amir Abd Rais[a,d], Mohd Natashah Norizan[a,d], Ili Salwani Mohamad[a,d] , and Sora-at Tanusilp[e]

[a]*Faculty of Electronic Engineering Technology, Universiti Malaysia Perlis (UniMAP), Arau 02600, Perlis, Malaysia*
[b]*Advanced Communication Engineering, Centre of Excellence (ACE), Universiti Malaysia Perlis (UniMAP), Kangar 01000, Perlis, Malaysia*
[c]*Centre of Excellence for Micro System Technology (MiCTEC), Faculty of Electronic Engineering Technology, Universiti Malaysia Perlis (UniMAP), Arau 02600, Perlis, Malaysia*
[d]*Center of Excellence, Geopolymer and Green Technology, School of Materials Engineering, Universiti Malaysia Perlis, Kompleks Pusat Pengajian Jejawi 2, Taman Muhibbah, 02600, Jejawi, Perlis*
[e]*Department of Electrical Engineering, Faculty of Engineering, Khon Kaen University, Khon Kaen 40002, Thailand*
**Corresponding author. Tel.: +604-9885509; fax: +604-9885510; e-mail: norfarhani@unimap.edu.my*

Received 30 Jun 2025, Revised 20 May 2026, Accepted 21 May 2026

ABSTRACT

The need to improve photovoltaic (PV) cell technology to enhance sustainability and efficiency has been underscored by the rising global demand for renewable energy. Because of their superior passivation quality and low-temperature fabrication, heterojunction (HJT) silicon PV cells are among the most promising options. However, the cells performance was limited due to recombination losses, suboptimal electric field distribution and structural inefficiencies. This study explores how HJT silicon PV cells can benefit from changes in geometry and doping configuration – including planar, columnar and pyramid – and examines their impact through Silvaco TCAD simulations. The properties studied are electric field patterns, hole and electron concentration and the pattern of carrier recombination. The results show that the planar design with the N-type top layer clearly exhibits the highest efficiency of 16.5247%, due to the uniform electric field, electron mobility, and low recombination rate of the N-type layer. A pyramidal shape can provide higher light-trapping ability and achieve a significant current density. But it incurs structural losses, and the electric field distribution is nonuniform, resulting in a lower cell fill factor (FF) and efficiency. The columnar configuration possesses weaker carrier collection at the vertical side walls, while it has strong local electric fields at the base. Among the others, this configuration has the lowest cell efficiency. The results show the significance of geometric accuracy and electric-field control in enhancing the performance of HJT cells. The study also highlights the balance required between the electrical performance and optical enhancement. This work paves the way for further research into novel geometries and enhanced structural integration in order to further optimize the efficiency of HJT cells.

Keywords: *Heterojunction, Solar cell, Photovoltaic cell, Silicon PV cell, Geometry modification*

1. INTRODUCTION

Solar panels, also known as Photovoltaic (PV) panels, play a vital role in the renewable energy revolution. They are acting as a pillar for sustainable energy sources. These sophisticated devices harness sunlight and convert it into electricity using the PV effect of PV cells. PV panels are classified into different generations based on their technological foundations and structural characteristics [1,2]. The first generation is based on traditional panels using crystalline silicon (c-Si), which can be divided into single-crystalline silicon (sc-Si) and multi-crystalline silicon (mc-Si) cells. The second generation is made of thin-film solar cells such as amorphous silicon (a-Si) and cadmium telluride (CdTe). The so-called next generation, or third generation, includes advanced technologies and innovative concepts such as organic or semi-organic photovoltaic panels (OPV), perovskite solar cells (PSC), dye-sensitised solar cells (DSSC), and quantum dot (QD) cells [3,4]. The PV cell is a crucial component of solar panels, and plays an important role in the conversion of sunlight into electricity. PV cells are usually made of semiconductor materials such as crystalline silicon, which are created to maximize the amount of sun absorbed and electric current produced [5,6]. Monocrystalline panels are manufactured using a single crystal structure and are very efficient. Polycrystalline panels feature multiple crystal structures, providing a compromise between efficiency and cost. Thin-film solar panels are made from thin layers of semiconductors and are flexible. They are commonly used in applications where traditional rigid panels are not desirable [7,8]. One of the major developments in the field of solar cells is the HJT silicon PV cell, a paradigm shift that combines traditional crystalline silicon technology with thin-film technology. This hybrid structure contains a thin layer of amorphous silicon (a-Si) or other suitable materials on both sides of the crystalline silicon wafer. Higher open-circuit voltage, better carrier collection, and lower recombination losses are examples of greater performance attributes [9]. On the other hand, by modifying the structure's geometry, a traditional silicon PV cell can be replicated as an HJT cell [10]. The performance optimization and improvement of HJT silicon solar cells are crucial for achieving the ever-evolving demand for clean and cost-effective energy solutions. Even with the developments, several challenges remain in HJT silicon PV cell technology, particularly in charge control, hole bending, electric field distribution, hole density, and geometric arrangement [11]. Efficiency improvement requires a uniform carrier distribution and precise electron charge. Meanwhile, the power generation is affected by irregular hole bending [12]. Moreover, the extraction efficiency of charge carriers and charge carrier mobility are greatly affected by the electric field distribution in the HJT layer [13,14].

Hence, understanding the relationship among material qualities, cell geometry, and electrical features is key. This study's main goals are to design and modify HJT silicon photovoltaic cells by changing their structural geometry, find and assess the geometric variations that yield the highest efficiency, examine the electric field for the best charge separation and transport mechanisms, and examine the electrical characteristics in terms of V_{OC}, J_{SC}, FF, and overall efficiency (η). The aim of the research is to address these challenges and limitations of HJT silicon PV technology, improve its performance, and investigate new solutions and optimization strategies.

To summarize, the goal of this study is to examine issues related to hole bending, hole density, electric field distribution, electron charge control and geometric arrangement in HJT Si photovoltaic cell. The goal of this research is to develop these cells further to higher performance levels, proposing creative solutions and optimization methods, particularly by altering the geometry of these cells. This would be a significant step forward in the development of low-cost and eco-friendly solar power systems.

2. BACKGROUND ON PHOTOVOLTAIC (PV) CELLS

PV devices apply the PV effect to convert solar radiation into electrical energy. Electron–hole pairs are produced when photons are absorbed in a semiconducting absorber layer. P–n junction diodes are found in traditional single-junction solar cells. Carrier separation is driven by an internal electric field, which allows charge collection at the appropriate electrodes and generates a photocurrent. The device's performance is determined by its current-voltage (I-V) characteristics under illumination; the contribution of photogenerated current is indicated by deviation from the dark I-V curve [7].

The short-circuit current density (J_{SC}), open-circuit voltage (V_{OC}), fill factor (FF), and maximum power output (P_{max}) are important variables. The device's overall power conversion efficiency (PCE) is determined by multiplying these three characteristics [5]. Efficiency is a crucial element in evaluating solar cell performance. Efficiency, calculated as the ratio of electrical power output to solar power input, includes several factors. Semiconductor material properties, surface passivation techniques, and intricate design considerations contribute to efficiency enhancement.

HJT PV cells offer numerous advantages over traditional designs. Combinations of materials, such as amorphous silicon (a-Si) and crystalline silicon (c-Si), create a more efficient interface for charge carriers and reduce energy losses [12]. The different bandgap energies of the two semiconductor materials enable more efficient absorption across a wider range of sunlight, thereby improving overall efficiency. Additionally, the HJT design helps reduce recombination losses and enhances the movement of charge carriers at the interface. [13].

3. METHODOLOGY

This study adopts a systematic methodology to design and optimize HJT silicon PV cells, using Atlas TCAD software's VWF Interactive Tools such as DeckBuild and TonyPlot. The physical and material parameters are approximately defined and compared with those reported in existing publications for validation [15]. A reference structure is used as a benchmark for comparison. The material parameters include N-type doped with phosphorus and P-type doped with boron. Ensuring that the simulation results are consistent with the reference article is crucial for confirming the software's functionality and reliability.

There are many different types of cell geometry designs for HJT silicon PV cells, including planar, columnar and pyramid. Meanwhile, the material parameters remain unchanged; only the top portion of the device is changed. The modified geometric structures are shown in Figure 1: planar, columnar, and pyramidal. A detailed investigation is conducted for each design, with the analysis varying across different structural parameters as detailed in Table 1. This analysis includes three variations: A) top region P-type and bottom region N-type; B) top region N-type and bottom region P-type; and C) variations in the height of the top region. These variations aim to optimize the placement and structure of the layers to improve charge carrier generation, separation, and overall cell efficiency.

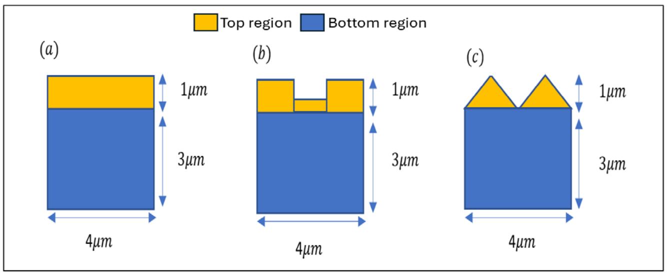

Figure 1. Geometrical dimension base for (a) planar, (b) columnar, and (c) pyramid structures.

Table 1. Variation of structural parameters for various geometrical structures

Structure	Variation	Doping (Top Region)	Doping (Bottom Region)	Height (Top Region)
Planar	A	P-type	N-type	1µm
	B	N-type	P-type	1µm
	C	N-type	P-type	0.5µm
Columnar	A	P-type	N-type	1µm
	B	N-type	P-type	1µm
	C	N-type	P-type	0.5µm
Pyramid	A	P-type	N-type	1µm
	B	N-type	P-type	1µm
	C	N-type	P-type	0.5µm

Understanding the structure of the mesh, region, electrode, and variables is crucial for designing the device's structure. To establish specific locations in microns for the vertical, horizontal, and depth lines, the mesh had to be defined accordingly for all three dimensions. Three mesh lines are required to design a 3D structure. These lines specify locations in microns and must be listed in the mesh statements as x-axis, y-axis and z-axis with coordinates [15]. The unit of measurement for the mesh is microns, and the default spacing is set to 1. Overlapping regions create new regions, and it is crucial to assign all mesh points within the structure to avoid errors in the Atlas Software. Doping in this simulation identifies the dopants used: boron and phosphorus. The anode and cathode were identified as essential for the electrodes. This identification is necessary to ground and extract the output in the Tonyplot graph. Next, the material is defined as silicon and referred to as a semiconductor component. The mesh, region, electrode, and doping parameters were defined accordingly, with variations for each structure. The electrical and PV characteristics of the designed cells were then analyzed using TonyPlot. Figure 2 shows the commands used to bias the solar cell to obtain its I-V characteristics. The final step involves optimizing the structure based on characterization results, aiming to identify the ideal configuration for maximum efficiency of an HJT solar cell.

```
#Post_Processing
extract init infile="DPlanar.log"
extract name="IV" curve(v."Anode",i."Cathode") outfile="curveIV.dat"
extract name="Jsc" y.val from curve(v."anode", i."cathode") where x.val=0.0
extract name="Voc" x.val from curve(v."Anode", i."Cathode") where y.val=0
extract name="Pm" max(curve(v."Anode",(v."Anode"* i."Cathode")))
extract name="Vm" x.val from curve(v."Anode",(v."Anode"* i."Cathode")) \
where y.val=$"Pm"
extract name="Im" $"Pm"/$"Vm"
extract name="FF" $"Pm"/($"Jsc"*$"Voc")
extract name="Eff" ($"Pm"/(4*(4)*(4)*1e-8*0.1))*100
tonyplot curveIV.dat
```

Figure 2. Commands to bias the solar cell for it's I-V characteristics.

4. RESULTS & DISCUSSION

4.1. Planar Structural Variations

The study investigated various planar, columnar, and pyramid geometry designs for HJT silicon PV cells to evaluate their baseline performances. Figure 3 illustrates the structural variations in the planar geometry, while Figure 4 presents their respective I–V characteristics. In Variation A, the cell adopts a P-type top region and an N-type bottom region, resulting in a V_{OC} of 0.381779 V, a J_{SC} of 2.79261×10^{-8} A/cm^2, and an efficiency of 12.0228%. The P-type emitter's reduced hole mobility (~400 cm^2/V·s) [16] and shorter minority-carrier lifetime enhance recombination losses near the front surface, which accounts for the minimal performance.

In contrast, Variation B changes the doping configuration with an N-type as the top region and a P-type as the bottom region. This changes lead to a noticeable improvement in performance with a V_{OC} of 0.390272 V, a J_{SC} of 4.1338×10^{-8} A/cm^2, and η of 16.5247%. The higher performance in this variation is supported by the superior electrical properties of N-type silicon, such as higher electron mobility (~1080 cm^2/V·s) [16] and longer minority-carrier lifetime. These factors support more effective charge collection and separation. Additionally, the band alignment at the HJT interface with the intrinsic and amorphous layers is improved by the front-side N-type emitter. As a result, recombination is reduced and electron extraction is more efficient.

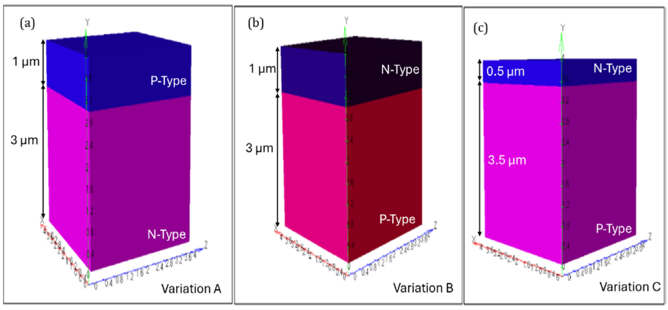

Figure 3. TonyPlot structure for planar geometry in (a) variation A, (b) variation B, and (c) variation C.

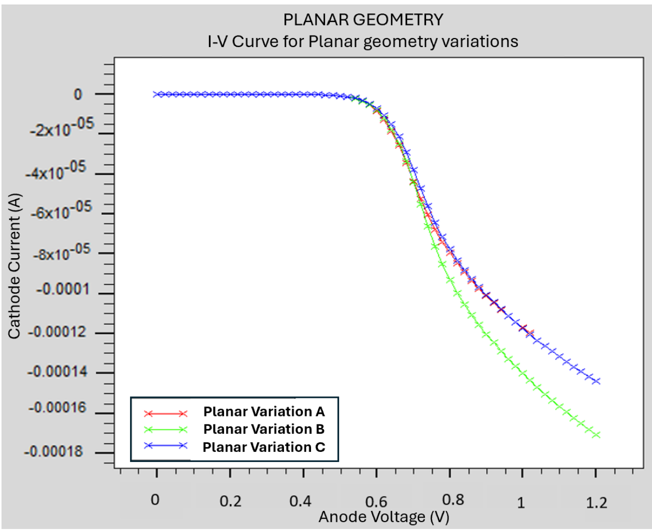

Figure 4. I-V Curve for planar geometrical variations.

Variation C adds a height adjustment to the top part, but maintains the N-type on top and P-type on bottom. This modification causes slight changes in the optical path length and the internal electric field distribution. This arrangement yields an efficiency of 15.4913%, a V_{OC} of 0.39286 V, and a J_{SC} of 3.93649×10^{-2} A/cm^2. The results illustrate that although the efficiency is marginally less than Variation B [1] due to the less stringent efficiency requirement, geometrical parameters such as the emitter height can have an impact on the carrier dynamics, optimizing the absorption of photons and minimizing the resistive losses. The advantage of an optimum doping arrangement is greater than the advantage of geometry optimization, however.

This discovery proves that the doping procedure has a big impact on cell performance. The N-type top emitter construction is shown to be superior to the P-type emitter construction. This is in line with theory, as N-type substrates and emitters would be ideally suited to high-efficiency HJT cell designs because of their better transport characteristics, degradation resistance and longer lifetimes [4]. Structural changes, such as changing the emitter thickness, provide another, less significant route to efficiency improvement via increased light absorption and increased carrier extraction.

4.2. Columnar Structural Variations

The framework for the variations in columnar geometry is shown in Figure 5. The I–V characteristics of their corresponding devices are plotted in Figure 6. Significant variations in electrical behaviour are evident from the analysis of these columnar structures, which are mainly influenced by the doping configuration and the columnar geometry's effects on carrier dynamics. Variation A's configuration yields a low efficiency of 4.82312%, a V_{OC} of 0.347362 V, and a J_{SC} of 1.23202×10^{-1} A/cm^2. The lower carrier transport from the P-type top and N-type bottom likely causes this poor performance. The recombination losses in the vertical column structure are larger because the hole mobility is lower and the diffusion length of the carriers is shorter. Also, if the vertical sidewalls are not adequately gathered, it can adversely affect the geometry.

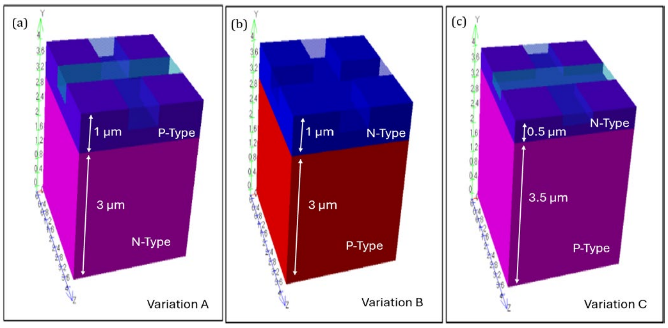

Figure 5. TonyPlot *s*tructure for columnar geometry in (a) variation A, (b) variation B, and (c) variation C.

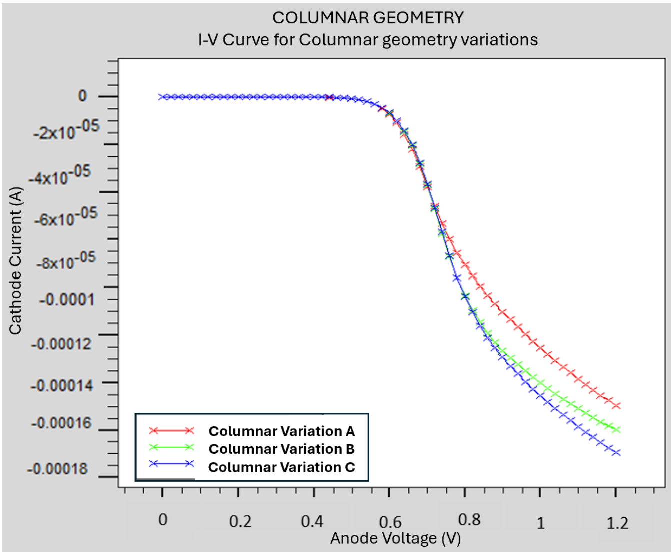

Figure 6. I-V Curve for columnar geometrical variations.

Variation B is a significant improvement, as it has a J_{SC} of 2.73491×10^{-1} A/cm^2, a V_{OC} of 0.379486 V, and an efficiency of 8.85678%. This enhancement points to an N-type top region doping setup that is more ideal. This arrangement contributes to increased collecting efficiency for the carriers and efficient electron transmission. A combination of the N-type emitter and columnar design gives rise to stronger built-in fields, greater vertical carrier separation, and reduced recombination at the column walls. Also, by increasing the optical path length, columnar structures can be used to enhance light trapping and, hence, J_{SC}.

With an efficiency of 7.68584%, Variation C produces a comparable V_{OC} of 0.379714 V but a somewhat lower J_{SC} of 2.63288×10^{-2} A/cm^2. This means that structural changes can lead to a less optimal electric field or increased parasitic resistance, even if the doping arrangement remains beneficial. Furthermore, it gives rise to an increase in interface recombination and a change in the local surface-to-volume ratio.

Of all the designs containing a column, Variation B is the most effective overall. This confirms the notion that the structure's geometry and the arrangement of doping will play a significant role in a device's performance. N-type emitters usually provide greater carrier mobility and stability. However, if one wants to enhance charge extraction and light trapping, then well-designed columnar structures are good. In such complex structures, it is difficult to control the diameters, and doping of the column profiles is crucial for reducing recombination and maximizing PV response.

4.3. Pyramid Structural Variations

The variation in pyramid geometry is shown in Figure 7. The I–V data of their corresponding is displayed in Figure 8. The results show the effect of the doping configuration on the pyramid geometry. The cell in Variation A records a V_{OC} of 0.400594 V, a J_{SC} of 1.32442×10^{-1} A/cm^2, and a low efficiency of 6.15031%. Although the pyramid has the highest V_{OC}, the J_{SC} was still low. In this configuration, with a P-type emitter on top. This means that the light is either not absorbed well or not removed from the carrier. This can occur due to a lack of field uniformity or increased recombination at the sharp edges of the pyramids [1]. The increased V_{OC} could be due to reduced dark current, and the low photocurrent limits the total power output.

Variation B, with a J_{SC} of 3.19062×10^{-2} A/cm^2, a V_{OC} of 0.380497 V, and an efficiency of 10.1412%, exhibits the highest performance among the pyramid structures. This variation has higher electron mobility, a longer minority carrier lifetime, and better band alignment for carrier separation. In this instance, the pyramid shape improves light trapping through multiple reflections. This improves photon absorption and lengthens the effective optical path. Additionally, well-passivated pyramid surfaces can reduce surface recombination. Additionally, it enables more efficient collection of photogenerated carriers. A significantly larger photocurrent is the reason for the relatively lower V_{OC} when compared to Variation A. As a result, overall power conversion efficiency improves.

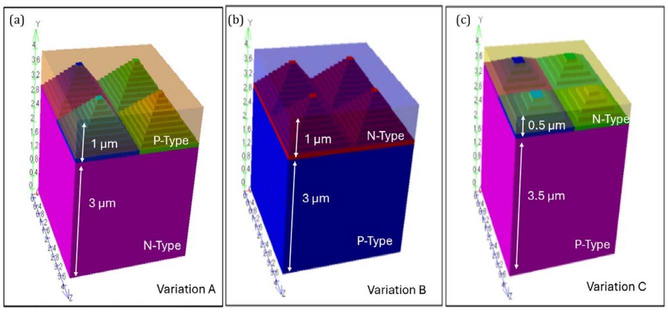

Figure 7. TonyPlot structure for pyramid geometry in (a) variation A, (b) variation B, and (c) variation C.

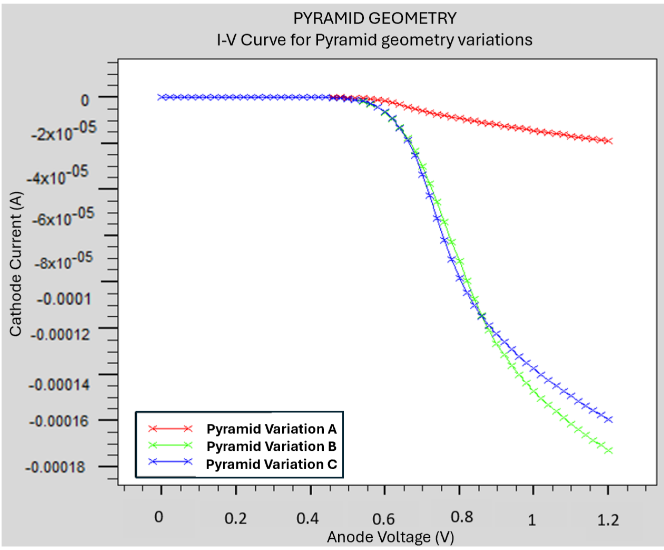

Figure 8. I-V Curve for pyramid geometrical variations.

While the pyramid height is changed to 0.5 µm, Variation C keeps the same doping setup as Variation B. It has an efficiency of 8.59313%, a V_{OC} of 0.380703 V, and a J_{SC} of 2.70427×10^{-2} A/cm^2. This geometric variation may have decreased the cell efficiency for light trapping and also introduced extra recombination at sharper corners or deeper trench regions. This resulted lower J_{SC}. The same V_{OC}, however, indicates that the doping gradient and electric field distribution are still conducive to charge separation.

Overall, Variation B is better than the other pyramid variations. This indicates that the geometric design of the pyramid structure and the optimization of the N-type emitter doping concentration are both important for making pyramid-based HJT solar cells more efficient. Numerous reflections inside the pyramids increase light absorption. They are effective only if they can be optimized structurally and adequately surface passivated. The results also confirm the overall improvement in the performance trend of N-type emitter designs, which is evident across all geometries, especially in those with enhanced optical and electrical routes.

4.4. Analysis Between Different Geometrical Structural Variations

Table 2 shows the performance of some HJT geometric and doping configurations of silicon PV cells. The interaction between optical enhancement and electrical activity is shown in the table below. With a J_{SC} of 4.1338×10^{-2} A/cm^2 V_{OC} of 0.390272 V, an FF of 0.655536, and a simulated efficiency of 16.5247%, the planar shape with an N-type top area outperforms the other designs. This higher performance can be attributed to the homogeneous electric field distribution shown in Figure 9, with a peak value of 9.17×10^3 V/cm near the connection. The field profile plays an important role in achieving good carrier separation throughout the active volume, decreasing recombination and promoting balanced transport [6]. On the other hand, the columnar geometry aimed to improve vertical carrier extraction, but it shows a low efficiency of 8.85678%. The theoretical advantage of vertical doping with respect to the field-aligned drift is compensated by the fact that, as simulated, the electric field is concentrated at the base of the columns. It reaches 2.18×10^4 V/cm; however, it drops rapidly along the column's sidewalls. This imbalance is the reason for weaker field forces on carriers being generated away from the base. This will increase the chances of recombination prior to the junction [11,16]. The structure's geometry can also lead to carrier crowding at the base. It also further increases recombination and internal resistance. The effects result in a lower J_{SC} of 2.73491×10^{-8} A/cm^2 and V_{OC} of 0.379486 V than the planar configuration. This indicates that the columnar electric field is strong but not strong enough to extract carriers consistently across the device.

Table 2 Summary of the electrical performances in different geometry variations

Structure	Variation	J_{SC} (A/cm^2)	V_{OC} (V)	FF	η (%)
Planar	A	2.79261×10^{-8}	0.381779 V	0.721711	12.0228
	B	4.1338×10^{-8}	0.390272 V	0.655536	16.5247
	C	3.93649×10^{-8}	0.39286 V	0.641095	15.4913
Columnar	A	1.23202×10^{-8}	0.347362 V	0.721288	4.82312
	B	2.73491×10^{-8}	0.379486 V	0.546156	8.85678
	C	2.63288×10^{-8}	0.379714 V	0.54954	7.68584
Pyramid	A	1.32442×10^{-8}	0.400594 V	0.741903	6.15031
	B	3.19062×10^{-8}	0.380497 V	0.534615	10.1412
	C	2.70427×10^{-8}	0.380703 V	0.534189	8.59313

Figure 9. The cross section and electric field distribution for variation B of geometry: (a)Planar (b)Columnar (c) Pyramid.

It has a textured surface, which improves light-trapping efficiency compared to a smooth surface. It has a relatively high J_{SC} (3.19062×10^{-2} A/cm^2), suggesting good photon absorption. However, the moderate efficiency of 10.1412% is limited by the low FF of 0.534615. An electric field simulation of the top part of the pyramid shows varying field strengths, particularly between the top and bottom. The presence of a strong electric field concentration at the edge of the pyramid and the underlying planar region is also noteworthy. This may be an important charge-collecting region. This punctuated thickening also indicates that the field is likely discontinuous across the structure and can help separate the carriers in the region.

Since the pyramid is made with a series of horizontal rectangular plates, the surface is not smooth. In these gaps, there are unexpected changes in potential and the electric field lines. These changes reduce effective carrier mobility at the sidewalls of the structure and at the interface, and increase interface recombination.

This finding indicates that by maximizing the surface area of the pyramid and columnar geometry can improve the light absorption. However, the non-uniform electric field distribution impacted the carrier transport behavior and collection efficiency of the cells. A better result can be achieved by making the structures more precise. Field continuation of engineering into the geometry transitions could result in consistent electric fields gradients and improved performance as well. Effective handling of the electric field, along with proper engineering and optimization of geometry, would be critical for making the most of 3D geometry in upcoming silicon PVs using HJT.

5. CONCLUSIONS

This study used numerical analysis and aim to determine the effect that planar geometry, columnar geometry and pyramid geometry having different doping levels on HJT silicon photovoltaic solar cells. Among all the three types, the planar geometry with the N-type top area was determined to perform better at 16.5247% efficiency rate. This is attributed to its even electrical properties, homogeneous distribution of electric fields and minimal recombination losses. However, during the intermediate process, its efficiency rate was 10.1412%, with improvements in light trapping and short-circuit current. This is mainly due to the presence of geometrical step changes, which affect the electric field, making it uneven. On the other hand, the columnar geometry performed poorly, achieving an efficiency of 8.85678%. This is attributed to local electric fields experienced in the vicinity of the column base and low light-absorption capacity. The smoothness and continuity of 3D designs, as well as the application of new materials, are central research areas that should be pursued in the future. In addition, incorporating experimental validation to relate the simulation to manufacturing reality. A cost-effective manufacturing capacity will also be crucial to scaling HJT technology up to become a viable and sustainable solar energy solution. It should be noted that the study's highest simulated efficiency of 16.5% is lower than the cutting-edge experimental HJT solar cells' 24–26% [4,6]. This discrepancy is caused by the assumptions made in the simulation, which are very simplified, such as non-optimised contact resistances, unoptimized material values, etc., and not the presence of sophisticated passivation layers. These factors reduce the simulated J_{SC} and FF in comparison with experimental prototypes. For this reason, in the future, more hand-made materials and surface passivation will be applied to fill this gap. This study is based on simulations, but the suggested shapes can be used with more sophisticated texturing and etching techniques. Practical implementation of the simulations is hindered by several problems, such as the minimization of interface defects, the passivation of surface in complicated 3D structures, and the uniformity of dopants. These obstacles must be overcome to translate the simulation results into devices.

ACKNOWLEDGMENTS

The authors would like to thank the support of the Fundamental Research Grant Scheme (FRGS) of the Ministry of Higher Education Malaysia with grant number FRGS/1/2023/STG07/UNIMAP/02/2.

REFERENCES

[1] Nayak, P. K., Mahesh, S., Snaith, H. J., Cahen, D.: Photovoltaic solar cell technologies: analysing the state of the art. In: *Nature Reviews Materials*, vol. 4, no. 4, pp. 269–285. Nature Publishing Group (2019)

[2] Muteri, V., Cellura, M., Curto, D., Franzitta, V., Longo, S., Mistretta, M., Parisi, M. L.: Review on life cycle assessment of solar photovoltaic panels. In: *Energies*, vol. 13, issue 1. MDPI AG (2020)

[3] Lin, H., et al.: Silicon Heterojunction Solar Cells with up to 26.81% Efficiency Achieved by Electrically Optimized Nanocrystalline-Silicon Hole Contact Layers. In: *Nature Energy*, vol. 8. Nature Publishing Group (2023)

[4] Danel, A., et al.: Closing the Gap between N- and P-Type Silicon Heterojunction Solar Cells: 24.47% Efficiency on Lightly Doped Ga Wafers. In: *Progress in Photovoltaics*, vol. 31, no. 12. Wiley (2022)

[5] Gholikhani, M., Roshani, H., Dessouky, S., Papagiannakis, A. T.: A critical review of roadway energy harvesting technologies. In: *Applied Energy*, vol. 261. Elsevier Ltd (2020)

[6] Hermle, M., Feldmann, F., Bivour, M., Goldschmidt, J. C., Glunz, S. W.: Passivating contacts and tandem concepts: Approaches for the highest silicon-based solar cell efficiencies. In: *Applied Physics Reviews*, vol. 7, issue 2. American Institute of Physics Inc. (2020)

[7] Taguchi, M.: Review—Development History of High Efficiency Silicon Heterojunction Solar Cell: From Discovery to Practical Use. In: *ECS Journal of Solid State Science and Technology*, vol. 10, no. 2, pp. 025002. The Electrochemical Society (2021)

[8] Haque, Md. M.: Investigating the Performance of Nanocrystalline Silicon HIT Solar Cell by Silvaco ATLAS. In: *Journal of Materials Science Research* (2019)

[9] Zhao, Y., Procel, P., Han, C., Cao, L., Yang, G., Özkol, E., Alcañiz, A., Kovačević, K., Limodio, G., Santbergen, R., Smets, A., Weeber, A., Zeman, M., Mazzarella, L., Isabella, O.: Strategies for realizing high-efficiency silicon heterojunction solar cells. In: *Solar Energy Materials and Solar Cells*, vol. 258. Elsevier (2023)

[10] Okil, M., Salem, M. S., Abdolkader, T. M., Shaker, A.: From Crystalline to Low-cost Silicon-based Solar Cells: a Review. In: *Silicon*, vol. 14, issue 5, pp. 1895–1911. Springer Science and Business Media B.V. (2022)

[11] Veirman, J., Leoga, A. J. K., Basset, L., Favre, W., Bonino, O., Le Priol, A., Rochat, N., Rouchon, D.: Understanding the Improvement of Silicon Heterojunction Solar Cells Under Light Soaking. In: *AIP Conference Proceedings*, vol. 2487. AIP Publishing (2022)

[12] Abd Rahim, A. F., Shamlan, M., Mohd Razali, N. S., Radzali, R., Mahmood, A., Hamzah, I. H., Abu Bakar, A.: Investigation of light trapping mechanism of Silicon solar cell performance utilizing Silvaco TCAD. In: *Journal of Physics: Conference Series*, vol. 1535, no. 1, pp. 012021. IOP Publishing (2020)

[13] Ponce, S., Li, W., Reichardt, S., & Giustino, F. (2020). First-principles calculations of charge carrier mobility and conductivity in bulk semiconductors and two-dimensional materials. *Reports on Progress in Physics.* doi:10.1088/1361-6633_ab6a43

[14] Hao, L., Zhang, M., Ni, M., Shen, X., & Feng, X. (2019). Simulation of a Silicon Heterojunction Solar Cell with a Gradient Doping Emitter Layer. *Journal of Electronic Materials*. doi:10.1007/s11664-019-07241-3

[15] Fang, Z., Xu, Z., Jang, T., Zhou, F., & Huang, S. (2020). Standard Deviation Quantitative Characterization and Process Optimization of the Pyramidal Texture of Monocrystalline Silicon Cells. *Materials*, 13(3), 564. doi:10.3390/ma13030564

[16] M. D. S. Basu and D. K. Bhattacharya, "New simplified model of back surface field polycrystalline silicon solar cells," *Modelling, Measurement & Control B*, vol. 110, no. 3, pp. 779–784, Jun. 2023, doi:10.18280/mmep.110302.